

Ultrasonic investigation of the Jahn-Teller effect in GaAs semiconductors doped by transition metals

N. S. Averkiev,^{1,a)} I. B. Bersuker,² V. V. Gudkov,^{3,4} K. A. Baryshnikov,¹ I. V. Zhevstovskikh,^{3,5} V. Yu. Mayakin,³ A. M. Monakhov,¹ M. N. Sarychev,³ V. E. Sedov,¹ and V. T. Surikov⁶

¹*Ioffe Physical-Technical Institute, 26 Polytekhnicheskaya, St.-Petersburg 194021, Russia*

²*Institute for Theoretical Chemistry, The University of Texas at Austin, Austin, Texas 78712, USA*

³*Ural Federal University named after the first President of Russia B. N. Yeltsin, 19 Mira, Ekaterinburg 620002, Russia*

⁴*Russian Vocational Pedagogical University, 11 Mashinostroiteley, Ekaterinburg 620012, Russia*

⁵*Institute for Metal Physics, Ural Division of Russian Academy of Sciences, 18 S. Kovalevskaya, Ekaterinburg 620990, Russia*

⁶*Institute of Solid State Chemistry, Ural Division of Russian Academy of Sciences, 91 Pervomaiskaya, Ekaterinburg 620990, Russia*

(Received 7 August 2014; accepted 30 August 2014; published online 11 September 2014)

Transition-metal-doped semiconductor GaAs crystals are used as model systems for spintronic research, as well as in other applications. To explore the structure and properties of such impurities, we extended the methodology of ultrasonic investigation of the Jahn-Teller effect in dielectric impurity-centers to the study of significantly different semiconductor impurities using the GaAs:Cu crystal as an example. Phase velocity and attenuation of ultrasound in this system were measured in the temperature interval of 1.9–80 K at 52 MHz and 156 MHz. The anomaly in the velocity and a peak of attenuation found for the longitudinal and slow shear waves indicate the presence of the Jahn-Teller effect with the e-type local distortions of the Cu_{Ga}4As impurity complex. The temperature dependence of the elastic modulus and relaxation time shows that below 5 K, the thermal activation mechanism of relaxation is possibly replaced by resonance type transitions. The main parameters of the Jahn-Teller effect, stabilization energy, minima positions and the barrier between them, frequency of pseudorotation of the distortions, and the tunneling splitting of the ground state energy, as well as the constant of exchange interaction between the two holes in Cu²⁺ centers and the concentration of the centers were estimated. © 2014 AIP Publishing LLC. [<http://dx.doi.org/10.1063/1.4895475>]

I. INTRODUCTION

Ultrasonic experiments have proved to be efficient in studying fundamental properties of various materials used in electronics, including semiconductors,¹ thermoelectric materials,² and ferroelectrics.³ Recent investigations of the III–V:3d and II–VI:3d crystals have demonstrated the possibility to obtain new information about the structure and properties of impurity centers, especially the parameters of the Jahn-Teller (JT) effect (JTE)⁴ (see Ref. 5 and references therein). Ultrasonic measurements reveal the active JT distortion modes, as well as several other characteristics of the adiabatic potential energy surface (APES) of the impurity center, including linear vibronic coupling constants, the symmetry of the distorted configurations, and the energy barrier between them, as well as the frequency of internal pseudorotations that determine high-temperature relaxations. This, in turn, allows one to reveal the mechanisms of relaxation and the temperature dependence of the relaxation time.

On the other hand, it was shown recently that among other important applications transition-metal-doped GaAs semiconductors serve as model systems for spintronic research.⁶ Obviously, transition metal impurities in this and

other semiconductor crystals are subjected to the JTE and/or the pseudo JTE,⁷ which may significantly influence their properties. To explore this possibility, the earlier worked out methods of ultrasonic investigation of the JTE in impurities in dielectrics may be useful. However, the extension of this approach to impurity centers in semiconductors is not straightforward. In distinction to wide-band-gap crystals, the physical properties of semiconductors are determined mainly by conduction electrons or holes that require a different theoretical description to take into account the free charge carriers. Therefore, the possibility to apply the local approach, used for dielectrics, to semiconductor impurities, even for small dopant concentrations, is not evident (see, e.g., Refs. 8 and 9).

To clarify this situation, we performed ultrasonic experiments on GaAs:Cu and GaAs crystals. These compounds have a band gap of ≈ 1.5 eV and the zinc-blende crystallographic structure. The Cu ion replaces Ga in its position in the tetrahedral surrounding by As ions. Earlier GaAs:Cu crystals were investigated by optical methods. The photoluminescence data¹⁰ revealed tetragonal distortions of the Cu_{Ga}4As centers along the $\langle 100 \rangle$ type axes. It was shown that elements of the group I in the Periodical system such as Cu, Ag, and Au substituting Ga in GaAs create deep centers with two holes coupled in the ground state.¹⁰ Theoretical

^{a)}Electronic mail: averkiev@les.ioffe.ru

considerations of the possible manifestation of the JTE in ultrasonic experiments on such systems reveal two possible effects: resonance and relaxation.¹¹ The effect of relaxation was observed in most of the experiments performed so far on systems with isolated JT centers starting with $\text{Al}_2\text{O}_3\text{:Ni}^{3+}$ (see Ref. 12). The relaxation effect is due to the changes in the distribution of local JT distortions produced by the ultrasonic wave. It manifests itself as a peak in the temperature dependence of ultrasonic attenuation and anomalies in the phase velocity that occurs at the point of transition from the isothermal to the adiabatic mode of ultrasonic propagation; it takes place at the temperature, where $\omega\tau \approx 1$ with ω as the cyclic frequency of the ultrasonic wave, and τ as the relaxation time.¹³ To the best of our knowledge, the resonant interaction predicted in Ref. 14 was reported only for GaAs:Mn^{15} seen as resonant transitions between the tunneling energy levels of the Mn center modified by random lattice imperfections.

In the present paper, we report the results of a rather full investigation of the Cu-doped GaAs semiconductor by studying all the ultrasonic normal modes propagating along the $\langle 110 \rangle$ crystallographic axis. The experimental conditions make it possible to determine all the elastic moduli of the cubic lattice and to find out what ultrasonic normal mode interacts with the local JT active mode reflecting the symmetry features of the global minima of the APES. In our preliminary investigation of GaAs:Cu performed in the interval 4.2–25 K, the peak of attenuation was found, and it was interpreted as of the relaxation origin.¹⁶ The active local mode proved to be of e type with the JT centers having tetragonal E distortions. The attenuation did not vanish when approaching the $T = 0$ K temperature, so it was assumed that there is a resonant component predicted earlier.¹¹ To support or refute this assumption, we performed extended ultrasonic measurements including not only the attenuation α , but also the phase velocity v measurement in a broadened interval of temperatures, 1.8–80 K. The data on phase velocity show that the observed anomalies can be interpreted mainly as relaxation in the JT centers. The temperature dependence of the relaxation time $\tau(T)$ revealed the dominant mechanisms of relaxation: thermal activation above $T \approx 10$ K and possible resonant transitions between the vibronic energy levels of the multimimum potential energy barrier at lower temperatures. The experimental data allowed us to estimate the magnitudes of the potential energy barrier between the minima $V = 14.5 \pm 0.5$ meV, the vibronic pseudorotational frequency⁴ $\nu_0 = (8.6 \pm 4.9) \times 10^{12}$ Hz, the radius of the APES minima trough⁴ $\rho = 0.13 \pm 0.01$ Å, the tunneling splitting of the ground state energy $\hbar\omega_0 \approx 15$ μ eV, the constant of exchange interaction $|\Delta| < 2$ meV between the two holes localized on the Cu^{2+} center and the concentration of these centers $n_{\text{JT}} = (5.4 \pm 0.3) \times 10^{17} \text{ cm}^{-3}$.

Note that the possibility to obtain the numerical values of the parameters of the JTE experimentally, provided by such ultrasonic investigation, is of much wider importance, as it may contribute essentially to revealing materials with bistabilities for electronics¹⁷ and in search for multiferroics.¹⁸

II. EXPERIMENT

A. Experimental details

Two samples used in our study, GaAs and GaAs:Cu, were prepared at the Ioffe Physical-Technical Institute. Initially, they were cut off one ingot of GaAs with the dimensions of approximately $8 \times 6 \times 4$ mm. The doping process was accomplished by diffusion from the surface during 58 h at the temperature of 1000 °C. The concentration of the dopant $n_{\text{Cu}} = (9.0 \pm 0.1) \times 10^{18} \text{ cm}^{-3}$ was determined by inductively coupled plasma mass spectroscopy using the ELAN 9000 (Perkin-Elmer SCIEX) facility. Experiments were carried out on the setup operating as a variable frequency bridge.¹⁹ The ultrasonic waves propagating along the $\langle 110 \rangle$ axis were generated and registered by LiNbO_3 piezoelectric transducers with the fundamental resonant frequency of about 52 MHz. The direction $\langle 110 \rangle$ was chosen because there are no degenerate normal modes propagating along such crystallographic axes, and all the non-vanishing elastic moduli c_{11} , c_{12} , and c_{44} can be measured.

Attenuation α and phase velocity v of the mode were determined by the corresponding elastic modulus, which we take as a complex variable $c_\beta : \alpha_\beta = \frac{1}{2}(\omega/v_\beta)(\text{Im}[c_\beta]/\text{Re}[c_\beta])$, $v_\beta = \text{Re}[(c_\beta/d)^{1/2}]$, where d is the density of the crystal. Index β denotes the type of the mode: one longitudinal ($\beta = l$) and two shear waves, namely, fast ($\beta = f$, polarization along $\langle 001 \rangle$) and slow ($\beta = s$, $\langle 1\bar{1}0 \rangle$). Accordingly, $c_l = (c_{11} + c_{12} + 2c_{44})/2$, $c_f = c_{44}$, and $c_s = (c_{11} - c_{12})/2$, where c_{11} , c_{12} , and c_{44} are nonzero components of the elastic moduli tensor in the cubic crystal. The presence of the c_{44} modulus in the expression for c_β indicates that the wave produces trigonal distortions of the tetrahedral complex $\text{Cu}_{\text{Ga}}4\text{As}$ (i.e., distortions along the $\langle 111 \rangle$ type axis), whereas the presence of c_s indicates tetragonal distortions (along $\langle 100 \rangle$). The expression for c_l can be introduced in terms of symmetry moduli c_f , c_s and $c_B = (c_{11} + 2c_{12})/3$, where c_B is the bulk modulus describing the totally symmetric distortions. Thus, the local E type mode manifests itself in attenuation and velocity of the slow shear and longitudinal waves, whereas the local T mode initiates the anomalies of the fast and longitudinal waves.

B. Results

The results of the measurements performed at 52 MHz are given in Figures 1–5. They show the peak of attenuation and the variation of the phase velocity typical for relaxation processes. This specific behavior is observed only for the slow shear and longitudinal ultrasonic waves confirming the tetragonal distortions of the $\text{Cu}_{\text{Ga}}4\text{As}$ centers, found earlier in photoluminescence experiments.¹⁰

C. Relaxation time

The method of the relaxation-time evaluation¹³ assumes that the peak in the temperature dependence of attenuation is due solely to the relaxations on the JT centers. In fact, there can be other mechanisms, and their relaxation contribution α_r should be extracted from the total attenuation α . Fortunately, most of other contributions have monotonic

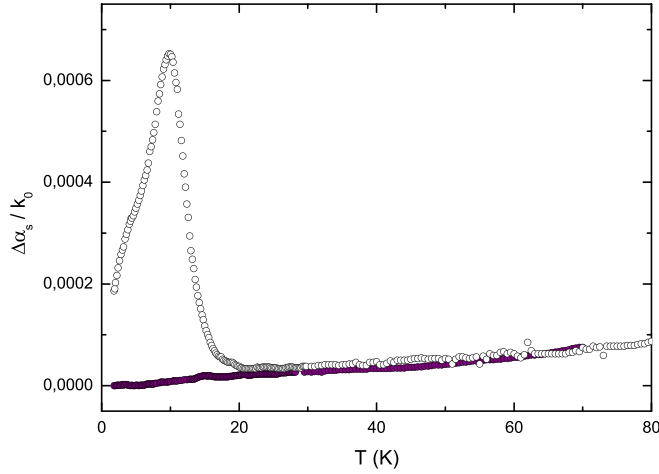


FIG. 1. Temperature dependences of relative attenuation of the 52 MHz ultrasonic slow shear wave propagating along the $\langle 110 \rangle$ crystallographic axis. Filled and unfilled symbols relate to GaAs and GaAs:Cu crystals, respectively. $\Delta\alpha_s = \alpha_s(T) - \alpha_s(T_0)$, $k_0 = \omega/v_0$, $v_0 = v_s(T_0)$, where $T_0 = 1.8$ K is the reference temperature. The curve related to GaAs:Cu is shifted to coincide with that of GaAs at high temperatures.

temperature dependences at low temperatures (see, e.g., the curve related to GaAs in Figure 1 or the one related to the fast shear mode in Figure 3). This simplifies the extraction of $\alpha_r(T)$. An example of such a procedure is shown in Figure 5. The background attenuation was simulated by the function $\alpha_b(T) = 3.63 \times 10^{-5} \times T^2$ and the measured curve $\alpha(T)$ was shifted to fit the curve $\alpha_b(T)$ at high temperatures. The difference $\alpha_r(T) = \alpha(T) - \alpha_b(T)$ represents contribution of the relaxation in the JT system to the total attenuation; it can be used for the evaluation of the relaxation time¹³

$$\tau = \frac{1}{\omega} \left[\frac{\alpha_r(T_1)T_1}{\alpha_r(T)T} \pm \sqrt{\left(\frac{\alpha_r(T_1)T_1}{\alpha_r(T)T} \right)^2 - 1} \right], \quad (1)$$

where ω is the cyclic frequency of the ultrasonic wave and T_1 is the temperature corresponding to the condition $\omega\tau(T_1) = 1$. It was shown¹³ that T_1 can be easily found from

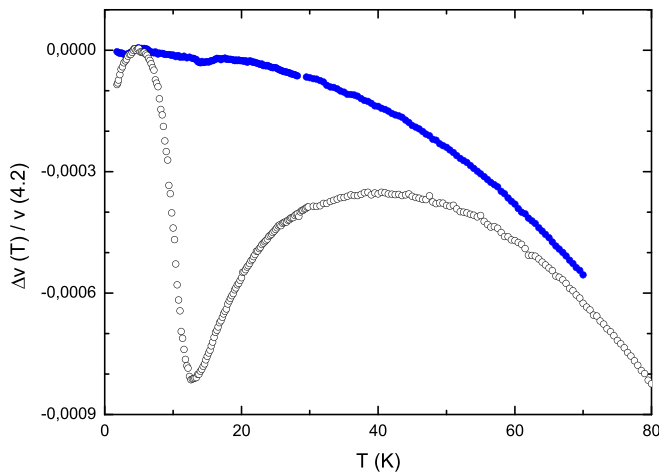


FIG. 2. Temperature dependences of the phase velocity of the 52 MHz ultrasonic slow shear wave propagating along the $\langle 110 \rangle$ crystallographic axis. Filled and unfilled symbols relate to GaAs and GaAs:Cu crystals, respectively. $\Delta v_s = v_s(T) - v_s(T_0)$, where $T_0 = 4.2$ K is the reference temperature.

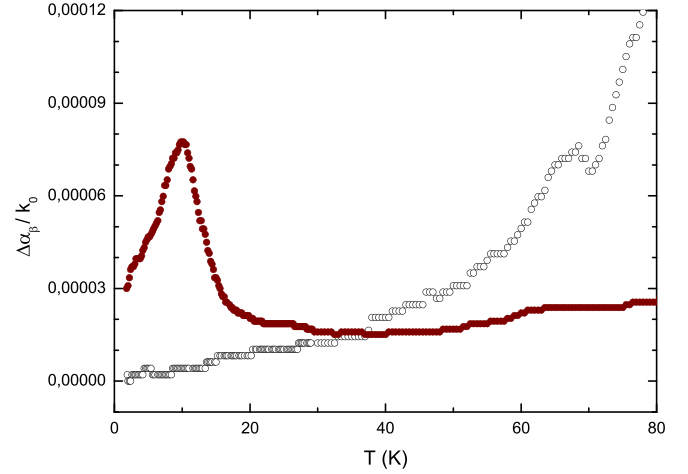


FIG. 3. Temperature dependences of the relative attenuation of the ultrasonic wave of 52 MHz propagating along the $\langle 110 \rangle$ crystallographic axis in GaAs:Cu. $k_0 = \omega/v_0$, $v_0 = v_\beta(T_0)$, where $T_0 = 1.8$ K is the reference temperature. Unfilled and filled symbols relate to the fast shear ($\beta=f$) and the longitudinal ($\beta=l$) waves, respectively, the latter being shifted for clarity.

the position of the peak in the temperature dependence of the curve $\alpha_r(T) \times T$. The dependences $\tau(1/T)$ calculated with the use of Eq. (1) for two frequencies of ultrasonic waves are given in Figure 6.

D. Relaxed and unrelaxed moduli

The temperature dependence of the relaxation time derived from the data on attenuation makes it possible to construct the temperature dependence of the relaxed c_s^R and unrelaxed c_s^U elastic moduli. The c_s^R value represents the low frequency limit of the dynamic (i.e., frequency dependent) modulus c_s , and c_s^U is its high frequency limit. If the system has only the relaxation process, discussed above and no others, the moduli c_s^R and c_s^U are the isothermal and adiabatic, respectively. The method of such presentation of $c_s^R(T)$ and $c_s^U(T)$ was introduced in Ref. 20 and discussed in detail in Ref. 13. The following formulas were used to

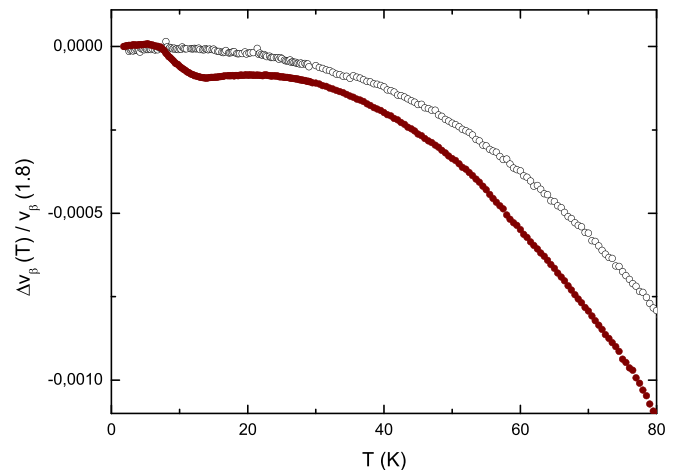


FIG. 4. Temperature dependences of the phase velocity of the ultrasonic wave of 52 MHz propagating along the $\langle 110 \rangle$ crystallographic axis in GaAs:Cu. $\Delta v_\beta = v_\beta(T) - v_\beta(T_0)$, where $T_0 = 1.8$ K is the reference temperature. Filled and unfilled symbols relate to the longitudinal ($\beta=l$) and the fast ($\beta=f$) shear waves, respectively.

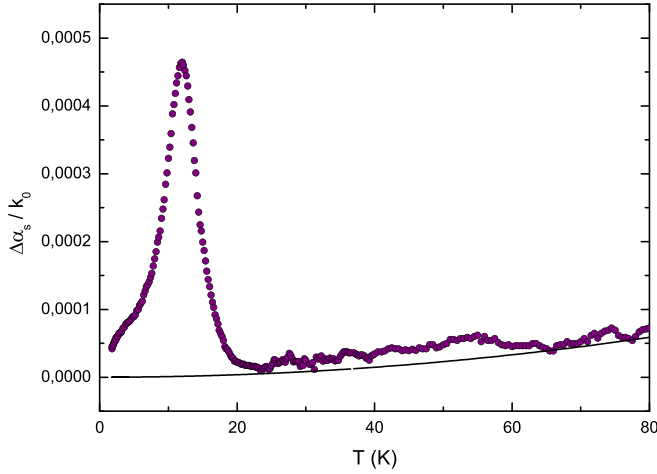


FIG. 5. Temperature dependence of relative attenuation of the 156 MHz ultrasonic slow shear wave propagating along the $\langle 110 \rangle$ crystallographic axis in GaAs:Cu. The background attenuation is presented by the solid line and defined as $\alpha_b(T) = 3.63 \times 10^{-5} \times T^2$.

determine the temperature variation of the moduli with respect to dynamic modulus c_s , which is defined at a reference temperature

$$\frac{c_s^U - c_0}{c_0} = 2 \frac{\Delta v_s}{v_0} + 2 \frac{\alpha_r}{k_0} \frac{1}{\omega \tau}, \quad (2)$$

$$\frac{c_s^R - c_0}{c_0} = 2 \frac{\Delta v_s}{v_0} - 2 \frac{\alpha_r}{k_0} \omega \tau, \quad (3)$$

where $c_0 = c_s(T_0)$, $v_0 = v_s(T_0)$, and $k_0 = \omega/v_0$. The curves obtained with the help of this procedure are given in Figure 7.

III. DISCUSSION

A. Relaxation

The peak of attenuation and the velocity anomaly are interpreted as being due to the relaxation process in isolated JT centers $\text{Cu}_{\text{Ga}}4\text{As}$. The influence of the relaxation process

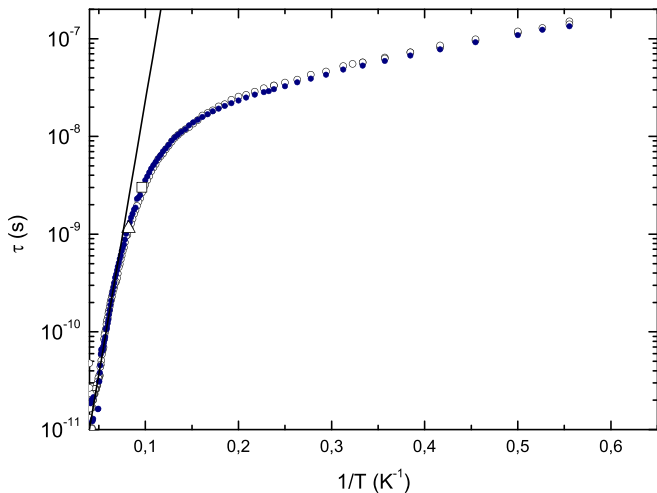


FIG. 6. Temperature dependence of the relaxation time constructed using the data on ultrasonic attenuation. Filled and unfilled circles relate to 52 MHz and 156 MHz, respectively, while the unfilled square and triangle indicate the values of τ at 52 MHz and 156 MHz under the condition $\omega\tau = 1$.

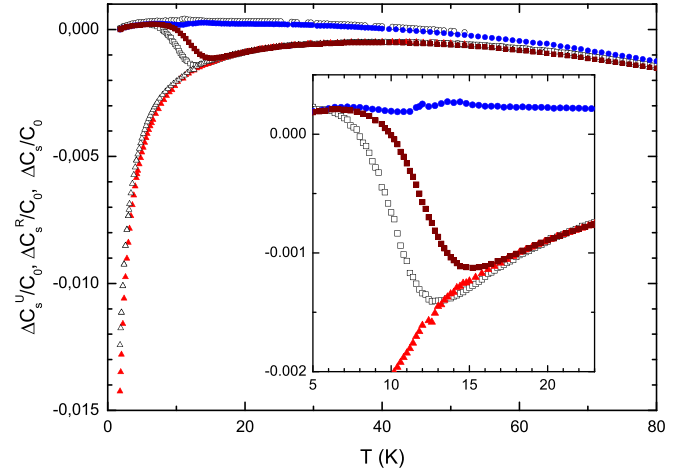


FIG. 7. Temperature dependences of the elastic moduli $\Delta c_s^U = c_s^U(T) - c_s^U(T_0)$, $\Delta c_s^R = c_s^R(T) - c_s^R(T_0)$ and $\Delta c_s = c_s(T) - c_s(T_0)$ in GaAs:Cu, where $T_0 = 1.8$ K. Unfilled and filled symbols are related to the 52 MHz and 156 MHz waves, respectively. Squares, triangles, and circles represent the dynamic (c_s), relaxed (c_s^R), and unrelaxed (c_s^U) moduli, respectively.

on the ultrasound propagation can be described within a phenomenological approach by the modified Hooke's law in which the time derivatives of stress and strain are expanded retaining only the lowest derivatives.²¹ For harmonic time-dependence of variables (i.e., stress and strain $\propto \exp(i\omega t)$) and small differences between the relaxed and unrelaxed moduli, the solution of the Zener equation for an arbitrary dynamic modulus c_β yields (see, e.g., Ref. 13)

$$c_\beta = c_\beta^U - \left(c_\beta^U - c_\beta^R \right) \frac{1 - i\omega\tau}{1 + (\omega\tau)^2}. \quad (4)$$

The expressions for the relative attenuation α_r/k_0 and phase velocity of the slow shear wave $\Delta v_s/v_0$ written in terms of elastic moduli and the frequency dispersion parameter $\omega\tau$ acquire the following form:

$$\frac{\alpha_r}{k_0} = \frac{1}{2} \frac{\text{Im}[c_s]}{c_0} = \frac{1}{2} \frac{(c_s^U - c_s^R)}{c_0} \frac{\omega\tau}{1 + (\omega\tau)^2}, \quad (5)$$

$$\frac{\Delta v_s}{v_0} = \frac{v_s - v_0}{v_0} = \frac{1}{2} \frac{\text{Re}[\Delta c_s]}{c_0} = -\frac{1}{2} \frac{(c_s^U - c_s^R)}{c_0} \frac{1}{1 + (\omega\tau)^2}. \quad (6)$$

Note that the harmonic dependence of the variables in the form of $\exp[i(\omega t - \mathbf{k}\mathbf{r})]$ assumes that $\alpha_s = -\text{Im}[k]$, where k is the complex wave number and in our consideration its imaginary part describes the attenuation of the amplitude not the energy. The factors dependent on $\omega\tau$ in Eqs. (5) and (6) are shown in Figure 8.

It can be seen that the relaxation attenuation has the maximum at $\omega\tau \approx 1$ and the phase velocity ($\text{Re}[c_s]$) transition from the isothermal to the adiabatic limits occurs at the same point. The equality is approximate because the value c_s^U is temperature independent and c_s^R is proportional to $1/T$.²⁰ So, $c_s^U - c_s^R \propto 1/T$ and the anomalies in $\alpha(T)$ and $v(T)$ are shifted to lower temperatures with respect to the temperature T_1 (see, e.g., Eq. (13) below and a similar treatment of ZnSe:Cr^{22}).

In our experiment, the increase of the ultrasound frequency shifts the peak of $\alpha_s(T)$ and minimum of $v_s(T)$ to

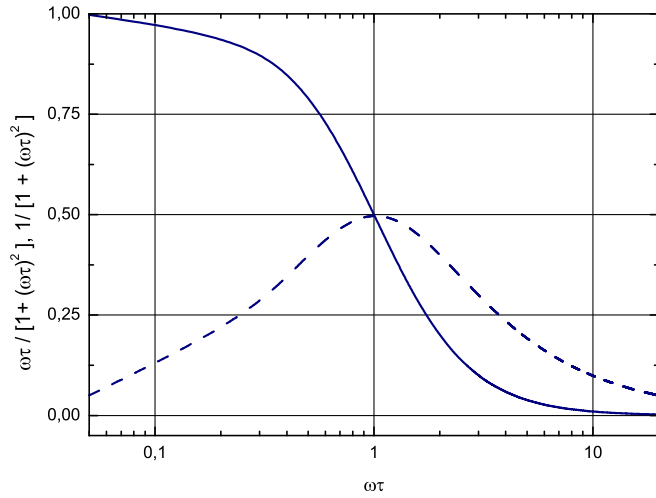


FIG. 8. The factors $\omega\tau/[1 + (\omega\tau)^2]$ (dashed curve) and $1/[1 + (\omega\tau)^2]$ (solid curve) as functions of the frequency dispersion parameter $\omega\tau$.

higher temperatures and decreases the relative variations of attenuation $\Delta\alpha_s/k_0$ (see Figures 1 and 5) and phase velocity $\Delta v_s/v_0$ (or elastic modulus $\Delta c_s/c_0 = 2\Delta v_s/v_0$ in Figure 7). This is why the non-monotonic variations of attenuation and velocity are considered as being due to the relaxation process.

Note that the relaxation mechanism is an intrinsic property of the crystal, which should be independent on the ultrasonic wave frequency. Therefore, the temperature dependence of the relaxation time is expected to be the same for different frequencies. This is indeed observed experimentally for the slow shear mode measured at 52 MHz and 156 MHz and shown in Figure 6: at high temperatures, the two curves $\tau(1/T)$ coincide, confirming that the underlying mechanism of the effect in this region is relaxation. However, at low temperatures, a small difference between these two curves emerges indicating that the frequency-independent relaxation mechanism is augmented by some additional processes. The same “irregularity” emerges in the temperature dependence of the phase velocity: the drop of $v_s(T)$ below 5 K (see Figure 2) cannot be explained in terms of relaxation. The suspicion falls on possible resonance absorption due to the transitions between the vibronic energy levels of the JT centers⁴ modified by the crystal imperfections (see the discussion below).

B. Potential energy barrier and vibronic (over the barrier) pseudorotation frequency

The slow variation of the relaxation time with temperature at low temperatures evidences for the tunneling mechanism of the relaxation. The tunneling occurs through the potential energy barrier between the JT minima of the APES. Above 10 K, we see the exponential dependence typical for the thermal activation process. The expression for the relaxation rate of this process for the $E \otimes e$ problem is given in Ref. 21

$$\tau^{-1} = 2\nu_0 \exp\left(-\frac{V_0}{k_B T}\right), \quad (7)$$

where ν_0 is the high-temperature limit of the frequency of pseudorotations of JT distortions, k_B is the Boltzmann

constant, and V_0 is the activation energy. Fitting this function to the curve $\tau = \tau(1/T)$ in the region of 15–18.2 K (shown by a line in Figure 6), it is possible to estimate the parameters $\nu_0 = 8.6 \times 10^{12}$ Hz and $V_0 = 11.2$ meV. The latter matches well the photoluminescence data (≈ 10 meV (Ref. 10)).

Note that the most of the parameters entering Eq. (13) (see below) are known with high accuracy due to the errors of the numerical evaluations of V_0 and ν_0 . The relative errors in estimation of k_0 and c_0 do not exceed 0.01. The main source of error for α_r is in the simulation of the temperature dependence of the background attenuation $\alpha_b(T)$. We evaluated this error as a half of the difference between the values obtained under the assumption that $\alpha_b(T)$ is a temperature-independent constant (equal to the attenuation at the temperature of the attenuation minimum at 52 MHz, $\alpha_b = \alpha(22\text{ K})$), and that for $\alpha_b(T) = 1.053 \times 10^{-5} \times T^2$. As a result, we get $V_0 = 11.2 \pm 0.5$ meV and $\nu_0 = (8.6 \pm 4.9) \times 10^{12}$ Hz. Figure 9 shows two versions of $\ln(\tau)$ obtained for the two α_b values mentioned above and the linear fit, which defines V_0 and ν_0 .

The potential energy barrier of the APES can be defined as $V = V_0 + E_0$, where E_0 is the energy of zero vibrations in the APES minima. Optical experiments and their theoretical analysis¹⁰ offered a number of calculated JTE parameters in GaAs:Cu. The nearest to our estimate of the potential energy barrier is $V = 14.3$ meV and $E_0 = 3.3$ meV. More accurate, the potential barrier evaluated in our experiment is $V = 14.5 \pm 0.5$ meV.

C. The adiabatic potential energy minima, exchange interaction constant, and tunneling splitting

Theoretical evaluation of the JTE in GaAs:Cu involves the exchange interaction between two holes located at the $\text{Cu}_{\text{Ga}}4\text{As}$ center¹¹

$$\hat{H}_{ex} = -\Delta(\hat{\mathbf{J}}(1) \cdot \hat{\mathbf{J}}(2)), \quad (8)$$

where Δ is the exchange interaction constant, and $\hat{\mathbf{J}}(i)$ is the operator of angular momentum of the i -th hole ($i = 1, 2$). In

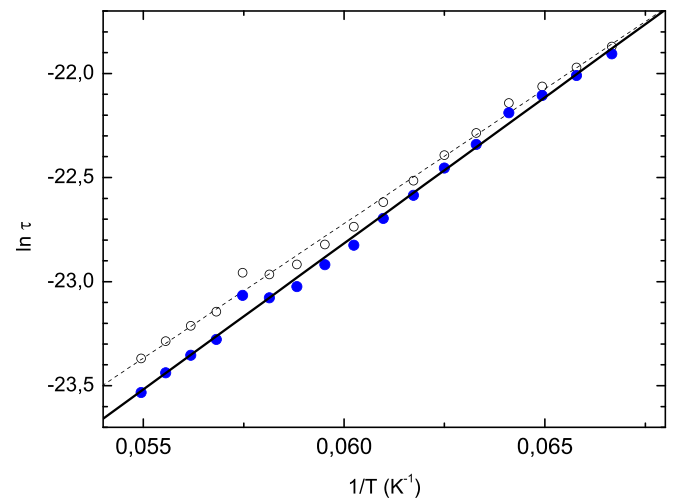


FIG. 9. Temperature dependence of relaxation time constructed using the data on the measured ultrasonic attenuation $\alpha(T)$ at 52 MHz and the two versions of the background attenuation α_b . Filled and unfilled symbols relate to $\alpha_b = \alpha(22\text{ K})$ and $\alpha_b(T) = 1.053 \times 10^{-5} \times T^2$, respectively.

fact, the vibronic coupling between the two states produced by the exchange interaction is a pseudo JTE.^{4,7} The expression for the lowest sheet of the APES in this case is (see Eq. (5) in Ref. 11)

$$\varepsilon = \frac{9}{4}\Delta - \sqrt{\frac{9}{4}\Delta^2 + F^2(q_2^2 + q_3^2)}, \quad (9)$$

where F is the linear vibronic coupling constant, $q_2 = 3Q_2/2$, $q_3 = 3Q_3/2$, and Q_2, Q_3 are the normal coordinates of the E type vibrations.⁴ With the quadratic vibronic coupling included the APES acquires three equivalent minima (see comments after Eq. (6) in Ref. 11) located at

$$\rho = \sqrt{q_2^2 + q_3^2} = \frac{F}{K} \sqrt{1 - \varepsilon^2}, \quad (10)$$

$$\Phi = \arctan \frac{q_3}{q_2} = \frac{\pi n}{3}, \quad n = 0, 2, 4, \quad (11)$$

where ρ and Φ are the polar radial and angular coordinates, respectively, K is the primary force constant (the force constant without the contribution of vibronic coupling) and ε takes into consideration the exchange interaction

$$\varepsilon = \frac{3K\Delta}{2F^2}. \quad (12)$$

The formulas for attenuation of ultrasound by these centers were derived for two mechanisms: relaxation and resonance. For the relaxation attenuation, the following expression was obtained:¹¹

$$\begin{aligned} \frac{\alpha_r}{k_0} &= \frac{1}{2} \frac{\Delta c_s}{c_0} \frac{\omega \tau}{1 + (\omega \tau)^2} \\ &= \frac{1}{2} \frac{n_{JT} b_T^2 [6\sqrt{1 - \varepsilon^2} + 1 + \varepsilon]^2}{64 c_0 k_B T} \frac{\omega \tau}{1 + (\omega \tau)^2}, \end{aligned} \quad (13)$$

where b_T is the potential-deformation constant and n_{JT} is the concentration of the JT centers (it differs from the impurity concentration since not all of them replace Ga ions in their positions). Equation (13) differs from one introduced in Ref. 11 by the factor 1/2. The discrepancy occurs because Eq. (30) in Ref. 11 describes attenuation of the energy, whereas in the present paper, we have introduced α as the imaginary part of the wave number, i.e., it describes the attenuation of the amplitude, which is twice smaller.

The expression for the concentration of the JT centers can be derived with the help of Eq. (13) written for $T = T_1$, which corresponds to the condition $\omega \tau(T_1) = 1$

$$n_{JT} = \frac{256 T_1 \alpha_r(T_1) c_0 k_B}{k_0 b_T^2 [6\sqrt{1 - \varepsilon^2} + 1 + \varepsilon]^2}. \quad (14)$$

The following magnitudes were used in the calculations below: $\alpha_r(T_1) = 0.80$ Np/cm, $T_1 = 10.4$ K, $b_T = -1.03$ eV,^{23,24} $v_0 = (c_0/d)^{1/2} = 2.48 \times 10^5$ cm/s, and $c_0 = 3.28 \times 10^{11}$ dyn/cm². The dimensionless parameter of the exchange interaction ε can be evaluated with the help of the expression for the stabilization energy in the linear JTE $E_{JT} = F^2/2K$.⁴ The exchange interaction between two holes localized on Cu_{Ga}4As impurity

complex modifies this expression to $E_{JT} = F^2(1 - |\varepsilon|)^2/2K$. The experimental data processed in the paper¹⁰ yield the value of $E_{JT} = 20$ meV at $\varepsilon = 0$. The exchange interaction diminishes the E_{JT} value, but the latter should not be less than the potential energy barrier for the thermal activation process, which was evaluated in our investigation as $V = 14.5$ meV. This value makes it possible to estimate $|\varepsilon| = 0.148$ as the upper limit.

From the analysis of Eq. (14), we obtained the concentration of the JT centers in the sample $n_{JT} = (5.4 \pm 0.3) \times 10^{17}$ cm⁻³. Using Eqs. (10) and (12) and the values of $F = 1.32 \times 10^7$ eV/cm and $K = 1.0 \times 10^{16}$ eV/cm² from Ref. 10, we get the following estimations: $\rho = 0.13 \pm 0.01$ Å and $|\Delta| = 2F^2|\varepsilon|/3K \leq 2$ meV. Note that n_{JT} proved to be smaller than the copper concentration $n_{Cu} = 9 \times 10^{18}$ cm⁻³. This fact evidences that only a small portion of the copper ions occupies Ga positions via diffusion from the sample surface.

The results obtained above made it possible to narrow the interval of admissible values of some JT parameters of the Cu_{Ga}4As impurity complex, including F , K , and the second order vibronic coupling constant G given in Ref. 10. Using these more accurate data, the value $|\varepsilon| = 0.148$, and Eq. (16) in Ref. 11, we can estimate the magnitude of the tunneling splitting of the ground state energy levels as $\hbar\omega_0 \approx 15$ μeV, or in frequency representation $\omega_0/2\pi \approx 3.7$ GHz. This value significantly exceeds the frequency of the ultrasonic waves used in our study (0.15 GHz). It means that direct transitions between the unperturbed tunneling energy levels cannot be realized in our experiment. However, we have indirect indication of the existence of some resonance type of attenuation: as seen from Figures 1, 2, 5, and 7, the curves below 5 K have a noticeable “shoulder” in the attenuation peak and a drop of the velocity and dynamic elastic modulus that are not seen in pure relaxation processes. Vibronic energy levels strongly affected by crystal imperfections that make the APES minima slightly different may be the source of these small low-temperature anomalies.

IV. SUMMARY

We extended the methodology of ultrasound exploration of the JTE in impurity centers in dielectrics to impurity centers in semiconductors important to a variety of applications in search for novel materials. By measuring the temperature dependence of attenuation and velocity of all the normal modes of the ultrasound waves propagating along the $\langle 110 \rangle$ axis of the GaAs:Cu crystal, we revealed the Jahn-Teller effect (JTE) in Cu_{Ga}4As impurity complexes. The JTE manifests itself in strong anomalies in the modes that generate tetragonal distortions in the $\langle 100 \rangle$ direction. Detailed analysis of the experimental data allowed us to show that the adiabatic potential energy surface contains three tetragonal minima typical for the $E \otimes e$ JTE problem, and to derive the numerical values of the main parameters of the JTE. Using an original method,¹³ we obtained the temperature dependences of the relaxation time $\tau(T)$ for both ultrasonic waves at 52 MHz and 156 MHz. Also we proved that the most of the

observed anomalies in the temperature dependences of attenuation and phase velocity are of relaxation origin. But at very low temperatures, the difference of the curves $\tau(T)$ obtained with different frequencies as well as the behavior of the dynamic and relaxed moduli makes it possible to assume that there is a contribution from resonant transitions between the vibronic energy levels in the minima of the APES perturbed by lattice imperfections.

The following Jahn-Teller parameters were evaluated: JTE stabilization energy $E_{JT} = 20$ meV, the energy barrier between the minima of the APES $V = 14.5 \pm 0.5$ meV, the vibronic frequency of the pseudorotations of the JT distortions $\nu_0 = (8.6 \pm 4.9) \times 10^{12}$ Hz, the numerical value of the coordinate of the distortion in the minima $\rho = 0.13 \pm 0.01$ Å, the exchange interaction constant between the two holes of the impurity $|\Delta| \leq 2$ meV, and the concentration of the JT centers $n_{JT} = (5.4 \pm 0.3) \times 10^{17} \text{ cm}^{-3}$. Based on the numerical values of the parameters of the JTE in $\text{Cu}_{\text{Ga}}4\text{As}$ impurity complexes, the magnitude of the tunneling splitting of the ground state energy levels was evaluated as $\hbar\omega_0 \approx 15 \mu\text{eV}$.

ACKNOWLEDGMENTS

The authors appreciate the financial support from Russian Foundation for Basic Research (Grant No. 12-02-00476-a). K. Baryshnikov is grateful for the financial support of the Dynasty Foundation. This work (N.S.A. and K.A.B.) was supported by the Government of Russia through the program P220 (Project No. 14.Z50.31.0021, leading scientist M. Bayer) and (V.V.G.) Ural Federal University Competitiveness Enhancement Program.

- ¹N. Nakamura, H. Ogi, and M. Hirao, *J. Appl. Phys.* **111**, 013509 (2012).
- ²S. Bhattacharya, A. M. Dehkordi, S. Tennakoon, R. Adebisi, J. R. Gladden, T. Darroudi, H. N. Alshareef, and T. M. Tritt, *J. Appl. Phys.* **115**, 223712 (2014).
- ³E. Smirnova, A. Sotnikov, S. Ktitorov, N. Zaitseva, H. Schmidt, and M. Weihnacht, *J. Appl. Phys.* **115**, 054101 (2014).
- ⁴I. B. Bersuker, *The Jahn-Teller Effect* (Cambridge University Press, Cambridge, 2006).
- ⁵V. V. Gudkov and I. B. Bersuker, "Experimental evaluation of the Jahn-Teller Effect parameters by means of ultrasonic measurements. Application to impurity crystals," in *Vibronic Interactions and the Jahn-Teller Effect*, edited by M. Atanasov, C. Daul, and P. L. W. Tregenna-Piggot (Springer, Dordrecht, Heidelberg, London, New York, 2012), pp. 143–161.
- ⁶T. Jungwirth, J. Wunderlich, V. Novak, K. Olejnik, B. L. Gallagher, R. P. Campion, K. W. Edmonds, A. W. Rushforth, A. J. Ferguson, and P. Nemec, *Rev. Mod. Phys.* **86**, 855 (2014).
- ⁷I. B. Bersuker, *Chem. Rev.* **113**, 1351 (2013).
- ⁸H. Tokumoto and T. Ishiguro, *J. Phys. Soc. Jpn.* **46**, 84 (1979).
- ⁹J. Zhaj-Yong, M. Shu-Hong, K. Xiao-Yu, and Z. Xian-Zhou, *J. Alloys Compd.* **475**, 70 (2009).
- ¹⁰N. S. Averkiev, A. A. Gutkin, E. B. Osipov, V. E. Sedov, and A. F. Tsatsulnikov, *Sov. Phys. – Solid State* **32**, 1546 (1990).
- ¹¹K. A. Baryshnikov, N. S. Averkiev, A. M. Monakhov, and V. V. Gudkov, *Phys. Solid State* **54**, 468 (2012).
- ¹²E. M. Gyorgy, M. D. Sturge, D. B. Fraser, and R. C. LeCraw, *Phys. Rev. Lett.* **15**, 19 (1965).
- ¹³V. V. Gudkov, "Ultrasonic consequences of the Jahn-Teller Effect," in *The Jahn-Teller Effect*, edited by H. Koppel, D. R. Yarkony, and H. Barentzen (Springer, Heidelberg, Dordrecht, London, New York, 2009), pp. 743–766.
- ¹⁴I. B. Bersuker, *Sov. Phys. – JETP* **17**, 1060 (1963); *Sov. Phys. – Solid State* **6**, 436 (1964).
- ¹⁵K. Lassmann and H. Schad, *Solid State Commun.* **18**, 449 (1976).
- ¹⁶N. S. Averkiev, K. A. Baryshnikov, I. B. Bersuker, V. V. Gudkov, I. V. Zhevstovskikh, V. Y. Mayakin, A. M. Monakhov, M. N. Sarychev, and V. E. Sedov, *JETP Lett.* **96**, 236 (2012).
- ¹⁷P. Garcia-Fernandez and I. B. Bersuker, *Phys. Rev. Lett.* **106**, 246406 (2011).
- ¹⁸I. B. Bersuker, *Phys. Rev. Lett.* **108**, 137202 (2012).
- ¹⁹V. V. Gudkov and J. D. Gavenda, *Magnetoacoustic Polarization Phenomena in Solids* (Springer, New York, Berlin, Heidelberg, 2000), pp. 25–27.
- ²⁰V. Gudkov, A. Lonchakov, V. Sokolov, I. Zhevstovskikh, and N. Gruzdev, *Phys. Status Solidi B* **242**, R30 (2005).
- ²¹M. D. Sturge, in *The Jahn-Teller Effect in Solids*, Solid State Physics Vol. 20, edited by F. Seitz, D. Turnbull, and H. Ehrenreich (Academic Press, New York, London, 1967), p. 137.
- ²²V. V. Gudkov, I. B. Bersuker, I. V. Zhevstovskikh, Y. V. Korostelin, and A. I. Landman, *J. Phys.: Condens. Matter* **23**, 115401 (2011).
- ²³E. B. Osipov, N. A. Osipova, M. E. Mokina, S. N. Tsvetkova, and S. D. Kangliev, *Semiconductors* **41**, 897 (2007).
- ²⁴N. S. Averkiev, Y. L. Ivanov, A. A. Krasivichev, P. V. Petrov, N. I. Sablina, and V. E. Sedov, *Semiconductors* **42**, 316 (2008).